LA-UR-15-20935
Approved for public release; distribution is unlimited.

Title: Comparison of Fast Neutron Detector Technologies

Author(s): Stange, Sy
Mckigney, Edward Allen

Intended for: Report

Issued: 2015-02-09

Comparison of Fast Neutron Detector Technologies

Sy Stange
Edward A. McKigney

February 3, 2015

Executive Summary

This report documents the work performed for the Department of Homeland Security Domestic Nuclear Detection Office as the project *Fast Neutron Detection Evaluation* under contract HSHQDC-14-X-00022.

This study was performed as a follow-on to the project *Study of Fast Neutron Signatures and Measurement Techniques for SNM Detection - DNDO CFP11-100 STA-01.* That work compared various detector technologies in a portal monitor configuration, focusing on a comparison between a number of fast neutron detection techniques and two standard thermal neutron detection technologies. The conclusions of the earlier work are contained in the report *Comparison of Fast Neutron Detector Technologies.*

This work is designed to address questions raised about assumptions underlying the models built for the earlier project. To that end, liquid scintillators of two different sizes–one a commercial, off-the-shelf (COTS) model of standard dimensions and the other a large, planer module–were characterized at Los Alamos National Laboratory. The results of those measurements were combined with the results of the earlier models to gain a more complete picture of the performance of liquid scintillator as a portal monitor technology.

List of Figures

List of Tables

1 Measurement Configuration and Considerations

This work was performed in order to address concerns raised about the assumptions made in *Study of Fast Neutron Signates and Measurement Techniques for SNM Detection* [1]. The concerns raised related to (a) the validity of the cost-parity technique used to compare liquid-scintillator-based detectors with ^{3}He-based detectors, and (b) the assumption made, regarding liquid scintillators, that the largest module routinely manufactured module demonstrated to achieve uniform efficiency over it's volume is a 3-inch-diameter by 3-inch-high right circular cylinder. In order to answer the questions raised, a measurement campaign was conducted using one 3-inch by 3-inch cylindrical liquid scintillator and one large-volume planar liquid scintillator. The objective was to use the results of this campaign to predict the performance of a liquid-scintillator-based portal, using performance for a given housing volume instead of cost-parity as a metric.

1.1 Detectors and Data Collection

One of the liquid scintillation detectors used for the measurements was a standard commercial-off-the-shelf (COTS) cylindrical detector manufactured by Scionix, with dimensions of 3 inches high by 3 inches in diameter. This detector was filled with EJ-309, which is a proprietary blend of organic solvents and fluors produced by Eljen Technologies. EJ-309 has been proposed as a replacement for standard liquid scintillators because it is far less flammable and maintains reasonable performance characteristics. The second detector was a large planar detector manufactured by Scionix, with dimensions of 25 cm $\times$ 25 cm $\times$ 10 cm deep. This detector was filled with EJ-301 (NE-213/BC-501A), which a very well-established xylene-based liquid. Both detectors are shown in Figure 1.1. The liquid scintillators and their data acquisition system were provided by the University of Michigan.

In addition to the two liquid scintillators, data was acquired with a SNAP neutron detector. This detector consisted of a single ^{3}He tube at a pressure of 10 atm surrounded by 2 inches of moderating polyethylene, a cadmium absorber and an additional inch of polyethylene shielding. The ^{3}He tube had a diameter of 1 inch and an active length of 4 inches. The SNAP also had a 1-inch-thick polyethylene shield that could optionally be attached to the front of the detector, in order to provide a ratio of counts measured with and without the shield. The SNAP is a very well-characterized and well-understood system, designed and built by LANL. [3] It outputs the efficiency for the user-specified

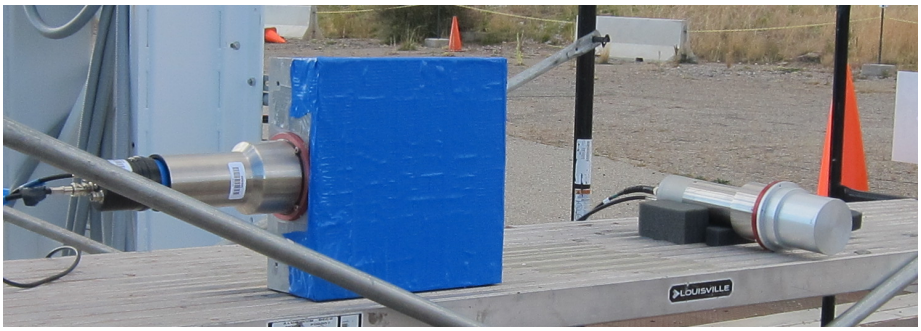

Figure 1.1: These measurements used two liquid scintillation detectors. On the left is the large planar detector; on the right is the standard cylindrical detector. They are shown here without the lead that surrounded them during measurements.

distance from the source, the number of neutrons detected during the preset measurement time, and a calculated neutron source strength.

The ^{252}Cf source measured was always placed at a distance of approximately 256.5 cm from the front of the liquid scintillator detector assembly (including any lead shielding in front of the detector). This distance approximates the center of a portal. Measurements were performed using the source alone, both unshielded and shielded by 5 cm of high-density polyethylene. Measurements were also performed using two standard 20-foot cargo containers. The container was positioned so that the source placement was at its center.

The measurement plan was designed to comply with ANSI standards for the testing of portal monitors, as laid out in the document, *American National Standard for Evaluation and Performance of Radiation Detection Portal Monitors for Use in Homeland Security* [2].

Output from the liquid scintillator data acquisition system consisted of:

- Total measurement time
- Total gamma-rays detected
- Total neutrons detected

In addition, the data acquisition output included the results of a processing algorithm that is under development:

- "True" gamma-ray rate
- "True" neutron rate

Among other things, the "true" rate algorithm attempts to compensate for pulses that were not analyzed because they ended outside the collection window. Full determination of errors for the "true" rates had not been integrated into the algorithm at the time of these measurement, making it impossible to assess the performance of the algorithm. It should be noted, though, that the percentage error of the "true" rates will not be lower than that of the measured rates, so nothing is lost by considering only the measured rates.

1.2 Data Analysis Process

For each of the three detectors (the SNAP and the two liquid scintillators), a three-step analysis process was conducted:

1. Using the total number of neutrons detected, determine the neutron detection rate for each measurement configuration.

2. Conduct a consistency check. Compare individual measurements of the source and container with the combined measurement of source and container:

   (Source + Container + Background) = (Source + Background) + (Container + Background) - Background.

   If these quantities are not statistically consistent, then the detector system is behaving anomalously.

3. If the detector system passes the consistency check, calculate the number of modules that could fit inside a standard portal (to build a same-detector-volume system) and use scaled count rates to build a Receiver Operating Characteristic (ROC) curve for the system.

1.2.1 Receiver Operating Characteristic Curves

The relationship between true and false positives is a key characteristic for portal detectors. If the probability of a false positive is high, relative to the probability of a true positive, then the passage of vehicles through the portal will be slowed by the need for secondary inspections. The relationship between these quantities can be shown as a function of the alarm threshold using a ROC curve.

For a measurement that is governed by Poisson statistics, the probability of measuring a number of neutrons, i, is

$$P(i,\mu) = e^{-\mu}\frac{\mu^i}{i!} \tag{1.1}$$

where μ is the mean number of neutrons detected. Therefore, if the alarm threshold is set to a number of neutrons t_n, the probability of an alarm is the sum of the probabilities of every number of neutrons greater than or equal to t_n.

$$P_{pos} = e^{-\mu}\sum_{i=t_n}^{\infty}\frac{\mu^i}{i!} \tag{1.2}$$

For the analysis of the measurements described in this report, we are interested in using Equation 1.2 to derive the probability for a true positive and the probability for a false positive. The probability of a false positive is a function of the mean rate of background neutrons μ_{bkg},

$$P_{fp}(t_n,\mu_{bkg}) = e^{-\mu_{bkg}}\sum_{i=t_n}^{\infty}\frac{\mu_{bkg}^i}{i!} \tag{1.3}$$

Similarly, the probability of a true positive, P_{tp}, is a function of the combined mean rates of signal neutrons, μ_{sig}, and background neutrons.

$$P_{tp} = e^{-(\mu_{sig}+\mu_{bkg})} \sum_{i=t_n}^{\infty} \frac{(\mu_{sig} + \mu_{bkg})^i}{i!} \tag{1.4}$$

Equations 1.5 and 1.6 will be used in this report when analyzing data from single detectors and from the SNAP-based portal. The measurements performed in this campaign indicated that a full-size liquid scintillator system (containing multiple modules of either the 3×3 or the planar liquid scintillator) will have μ_{bkg} and μ_{sig} greater than 120 n/s. In this regime, the Stirling approximation must be incorporated into Equations 1.5 and 1.6 in order for their results to be machine-calculable.

$$P_{fp}(t_n, \mu_{bkg}) = e^{-\mu_{bkg}} \sum_{i=t_n}^{\infty} \frac{\mu_{bkg}^i}{\sqrt{2\pi} i^{i+1/2} e^{-i}} \tag{1.5}$$

$$P_{tp} = e^{-(\mu_{sig}+\mu_{bkg})} \sum_{i=t_n}^{\infty} \frac{(\mu_{sig} + \mu_{bkg})^i}{\sqrt{2\pi} i^{i+1/2} e^{-i}} \tag{1.6}$$

2 Analysis of SNAP Detector

2.1 Background Measurements

The results of the background measurements are shown in Table 2.1. Measurements were performed both with and without the removable 1-inch polyethylene front shield.

2.2 Configuration Rates and Consistency Check

Results of the measurements of the containers and of the source alone are shown in Table 2.2. For each configuration, the goal was to collect two 30-minute measurements from the SNAP, one with the additional polyethylene shield and one without. However, on the final day of measurements, the SNAP malfunctioned (likely due to high humidity). Since time was limited and the liquid scintillator measurements had a high priority, the liquid scintillator measurements were continued while a new SNAP was located and delivered. This resulted in the loss of two measurements, which are marked with N/A in Table 2.2.

If a neutron detector functions correctly, we expect that the rate measured for a neutron source inside the container should be equal to the sum of the rates measured for the container alone and for the source alone, minus the background (since the background is present in both of the individual measurements). The presence of a container does not significantly suppress the neutron background. Table 2.3 shows that the single and combined measurements agree in all cases.

2.3 SNAP-based Portal and ROC Curve

The SNAP results may be used to predict the performance of a ^{3}He-based portal monitor system. This system would consist of two pillars, each containing two tubes of the same diameter and fill pressure as the SNAP detector. The tube length would be increased to 193 cm, equivalent to 19 of the tubes used in the SNAP. The predicted counts, based on those shown in Table 2.2 and assuming a 2.5-second transit time, are shown in Table 2.4.

Rate (s^{-1}) No Shield	Rate (s^{-1}) Shield
0.16 ± 0.009	0.12 ± 0.008

Table 2.1: Background rates measured for the SNAP detector

Container	Source?	Poly	No Shield Neutron Rate (s^{-1})	Shield Neutron Rate (s^{-1})
1	N	N	0.14 ± 0.009	0.12 ± 0.008
1	Y	Y	0.42 ± 0.02	0.27 ± 0.01
1	Y	N	0.40 ± 0.01	N/A
2	N	N	0.12 ± 0.008	0.11 ± 0.008
2	Y	Y	0.35 ± 0.01	0.25 ± 0.01
2	Y	N	N/A	0.27 ± 0.01
none	Y	Y	0.35 ± 0.01	0.22 ± 0.01
none	Y	N	0.37 ± 0.01	0.29 ± 0.01
Background			0.16 ± 0.009	0.12 ± 0.008

Table 2.2: Neutron rates measured by the SNAP detector. For measurements marked with N/A, no data was collected due to detector malfunction.

Container	SNAP Shield?	Source Shielded?	Single Measurement	Combined Measurements	Agree?
1	N	N	0.40 ± 0.01	0.35 ± 0.02	Y
1	N	Y	0.42 ± 0.02	0.33 ± 0.02	Y
1	Y	Y	0.27 ± 0.01	0.22 ± 0.02	Y
2	N	Y	0.35 ± 0.01	0.33 ± 0.02	Y
2	Y	N	0.27 ± 0.01	0.28 ± 0.02	Y
2	Y	Y	0.25 ± 0.01	0.21 ± 0.02	Y

Table 2.3: Comparison of neutron rates measured by the SNAP detector for container and source together ("Single Measurement" with rates measured for container and source separately ("Combined Measurements"). The single and combined measurements are within 3σ of one another in all cases.

Container	Source?	Poly	No Shield Neutrons	Shield Neutrons
1	N	N	26.6 ± 5.16	22.8 ± 4.77
1	Y	Y	79.8 ± 8.93	51.3 ± 7.16
1	Y	N	76.0 ± 8.72	N/A
2	N	N	22.8 ± 4.77	20.9 ± 4.57
2	Y	Y	66.5 ± 8.15	47.5 ± 6.89
2	Y	N	N/A	51.3 ± 7.16
none	Y	Y	66.5 ± 8.15	41.8 ± 6.46
none	Y	N	70.3 ± 8.38	55.1 ± 7.42
Background			30.4 ± 5.51	22.8 ± 4.77

Table 2.4: Predicted neutron counts measured by a ^{3}He-based portal monitor system.

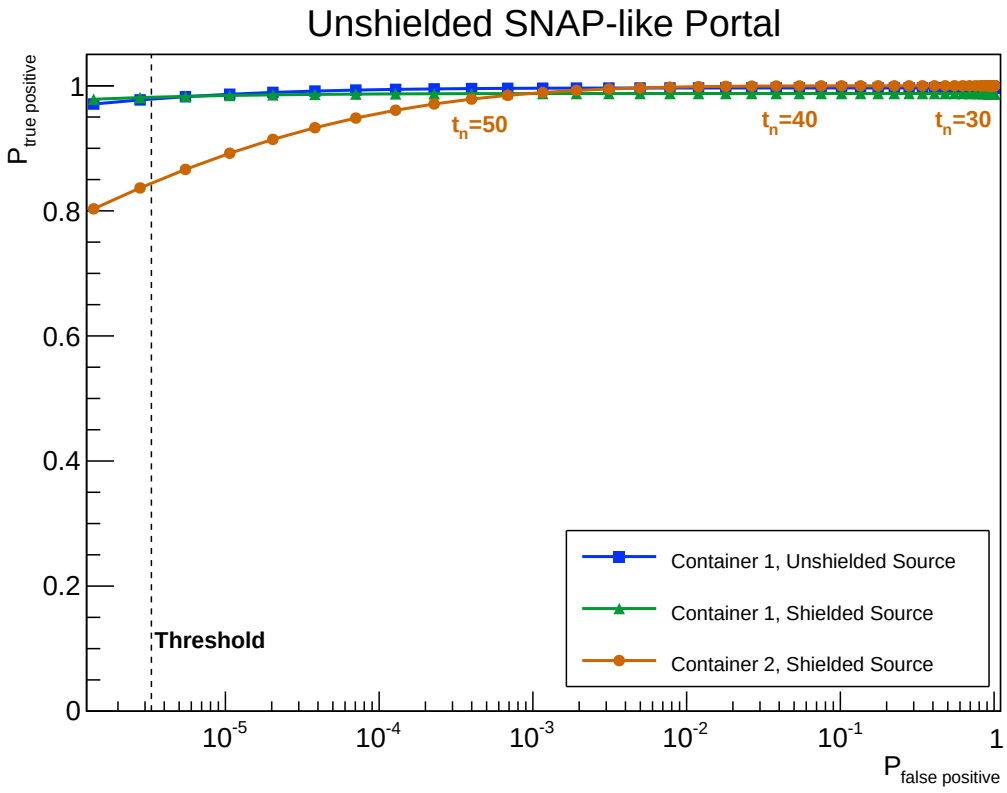

Figure 2.1: ROC curve for a ^{3}He-based portal monitor system based on the unshielded SNAP detector

ROC curves for portal monitors based on the unshielded and shielded SNAP detector, calculated using the counts given in Table 2.4, are shown in Figures 2.1 and 2.2, respectively. The system based on the unshielded SNAP clearly has better performance than the system based on the shielded SNAP.

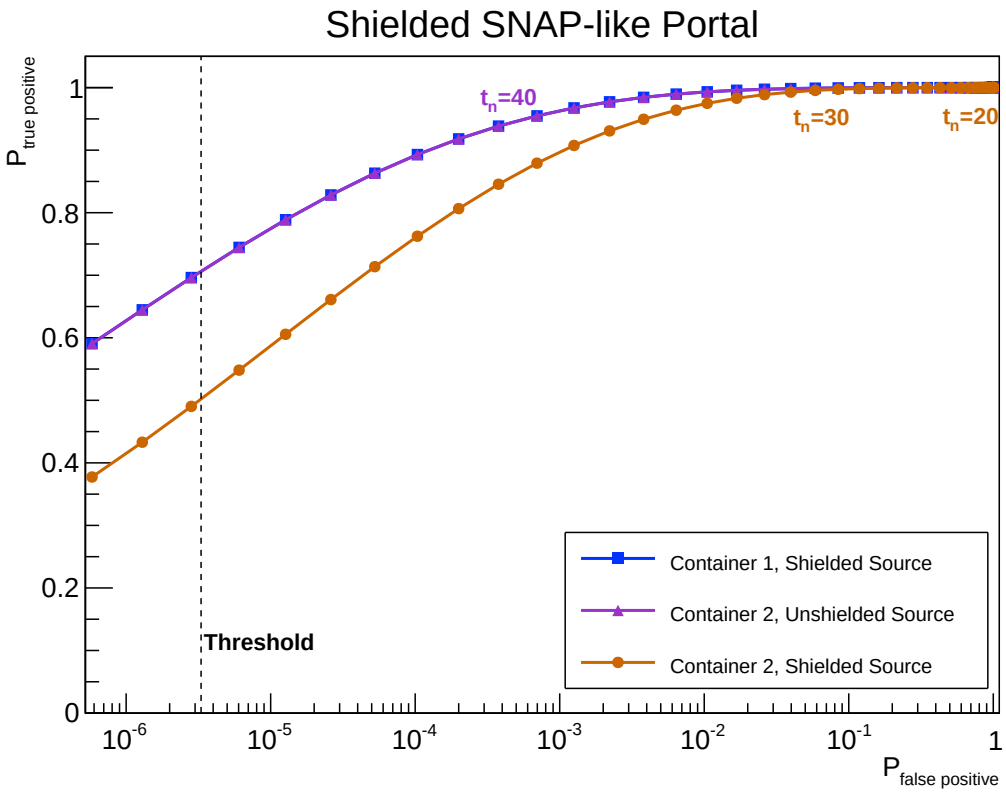

Figure 2.2: ROC curve for a ^{3}He-based portal monitor system based on the shielded SNAP detector

3 Analysis of Cylindrical Detector

3.1 Background Measurements

The results of background measurements are shown in Table 3.1. Note that the third measurement differs in a statistically significant way from the other two. The weather on the final day of measurements was overcast, indicating different humidity from the other days.

The observed background at the measurement site (∼7500 ft above sea level) was anticipated to be higher than the background routinely observed in Ann Arbor (∼800 ft). The University of Michigan team reported that the backgrounds they observed from both the cylindrical and planar detectors were about four times higher than they were accustomed to seeing, which is consistent with the experience of the LANL team.

3.2 Gamma-Ray Classification

One measurement was performed with only a ^{137}Cs gamma-ray source. The measured neutron rate was 1.17 ± 0.0255 neutrons/s. Unfortunately, due to time constraints no background was acquired on the day (20 October) when this measurement was taken, but it is consistent with the background taken on the following day. Based on this, it appears that the pulse shape discrimination algorithm worked well for this isotope/detector configuration and that the background measured on 20 October was statistically consistent with the background measured on 21 October.

3.3 Configuration Rates and Consistency Check

The neutron and gamma-ray detection rates are shown in Table 3.2. In-depth analysis of the gamma-ray rates is outside the scope of this report, but one interesting feature is the discrepancy in the effect of the polyethylene shield. In general, it is expected that the

Date	Time (s)	Rate (s^{-1})
16 Oct 14	3600	1.25 ± 0.0186
17 Oct 14	900	1.28 ± 0.0377
21 Oct 14	1800	1.15 ± 0.0253

Table 3.1: Background rates measured for the cylindrical detector

Container	Source?	Poly?	Bkg	Neutron Rate (s^{-1})	Gamma Rate (s^{-1})
1	N	N	2	1.30 ± 0.0269	37.2 ± 0.144
1	Y	Y	2	1.70 ± 0.0308	37.5 ± 0.144
1	Y	N	2	1.93 ± 0.0327	38.7 ± 0.147
2	N	N	2	1.16 ± 0.0254	44.9 ± 0.158
2	Y	Y	2	1.44 ± 0.0283	45.5 ± 0.159
2	Y	N	2	1.76 ± 0.0313	45.4 ± 0.159
none	Y	Y	1	1.54 ± 0.0292	21.16 ± 0.108
none	Y	N	1	2.03 ± 0.0336	22.31 ± 0.111
Background 1				1.25 ± 0.0186	21.1 ± 0.0765
Background 2				1.15 ± 0.0253	20.5 ± 0.107

Table 3.2: Neutron and gamma-ray rates measured by the cylindrical detector for two containers

addition of a ^{252}Cf source to the system will increase both the neutron and the gamma-ray (albeit to a lesser extent) count rates. For Container 1, the addition of the shielded ^{252}Cf source increased the measured gamma-ray rate by 0.8%, which is within the standard 3σ uncertainty of the container-only gamma-ray rate. For Container 2, on the other hand, the addition of the shielded ^{252}Cf source increased the measured gamma-ray rate by 1.3%, which is 4σ away from the original rate. More interesting, removing the poly shielding from the source had no significant effect on the measured gamma-ray rate for Container 2, but did have a significant effect for Container 1.

The rates measured for the combined source, container, and background are compared with the individual measurements of these quantities in Table 3.3. Since different backgrounds were measured for the source alone and for the container measurements (as indicated in Table 3.2), the expression used for the combined rate must take this into account. The measurements are combined as

$$R_{source} + R_{bkg2} + R_{cont} = (R_{cont} + R_{bkg2}) + (R_{source} + R_{bkg1}) - R_{bkg1} \tag{3.1}$$

where the parentheses indicate rates measured together as a single measurement. Table 3.3 shows that for all of the scenarios, the single and combined measurements agree to within three standard deviations.

3.4 Cylinder-Based Portal and ROC Curve

We are able to fit 24 3-inch by 3-inch liquid scintillator modules into each side of a standard portal. Predicted counts, as calculated using the values in Table 3.2, for a transit time of 2.5 seconds through portal using a total of 48 cylindrical detectors are shown in Table 3.4.

ROC curves for this system are shown in Figure 3.1. Performance of the portal based on the 3-inch by 3-inch liquid scintillator is clearly better for an unshielded source than for a

Container	Poly?	Single Measurement	Combined Measurements	Agree?
1	N	1.93 ± 0.033	2.08 ± 0.047	Y
1	Y	1.70 ± 0.031	1.59 ± 0.044	Y
2	N	1.76 ± 0.031	1.94 ± 0.046	Y
2	Y	1.44 ± 0.028	1.45 ± 0.043	Y

Table 3.3: Comparison of neutrons rates measured with the cylindrical liquid scintillator for container and source together ("Single Measurement" with rates measured for container and source separately ("Combined Measurements").

Container	Source?	Poly?	Neutrons
1	N	N	156.0 ± 12.49
1	Y	Y	204.0 ± 14.28
1	Y	N	231.6 ± 15.22
2	N	N	139.2 ± 11.80
2	Y	Y	172.8 ± 13.14
2	Y	N	211.2 ± 14.53
none	Y	Y	184.8 ± 13.59
none	Y	N	243.6 ± 15.61
Background 1			150.0 ± 12.25
Background 2			138.0 ± 11.75

Table 3.4: Projected neutron counts for a portal using 48 3"×3" liquid scintillators and a vehicle transit time of 2.5 seconds

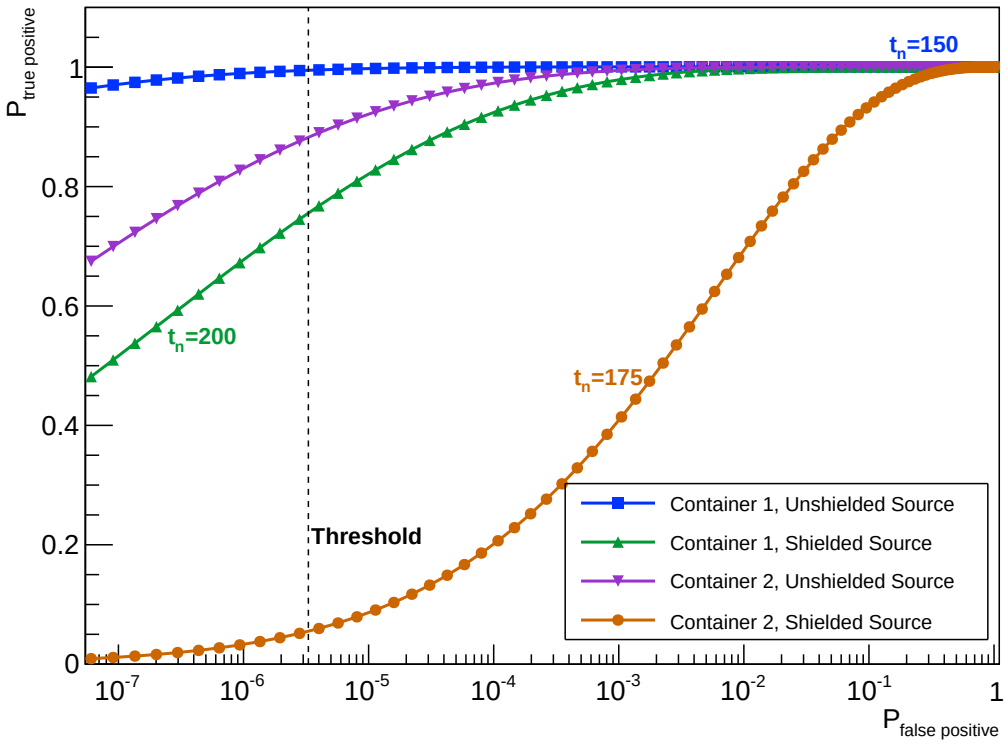

Figure 3.1: ROC curves for a portal monitor system based on the 3-inch by 3-inch liquid scintillator

shielded source.

4 Analysis of Planar Detector

4.1 Background Measurements

The results of background measurements are shown in Table 4.1. There was no statistically significant variation in the background, so the background on the final day of measurements, 4.33 ± 0.0491 n/s, was assumed to be the applicable background in all cases.

The measurement configuration for the planar detector called for a large amount of lead surrounding the detector. Due to concerns regarding the potential increase in background due to spallation, on the final day of measurements a background measurement was performed without the lead. Unexpectedly, this showed a 75% increase in the neutron background (an effect not shown by the cylindrical liquid scintillator).

4.2 Gamma-Ray Classification

The neutron rate measured from the paddle in the presence only of a ^{137}Cs source was 4.43 ± 0.0351 n/s. This neutron rate was statistically consistent with the background rate of 4.44 ± 0.0703 n/s on the day of measurement, indicating that the gamma-ray misidentification for this detector was very low for the energy for gamma-rays with energies at or below 662 keV.

4.3 Configuration Rates and Consistency Check

The neutron and gamma-ray detection rates are shown in Table 4.2. Several of the neutron rates merit further discussion. First, the rate of 3.97 n/s measured for Container 1 alone is lower than the background by a statistically significant amount. Second, the rate of 7.14 n/s measured for Container 2 alone is higher than the background by a statistically significant amount. Since a container by itself does not significantly suppress or contribute

Date	Time (s)	Rate (s^{-1})	Note
16 Oct 14	7200	4.24 ± 0.024	
17 Oct 14	900	4.44 ± 0.070	
21 Oct 14	1800	4.33 ± 0.049	
21 Oct 14	1800	7.63 ± 0.021	no lead

Table 4.1: Background rates measured for the planar detector

Container	Source?	Poly?	Neutron Rate (s^{-1})	Gamma Rate (s^{-1})
1	N	N	3.97 ± 0.0332	492.1 ± 0.4
1	Y	Y	6.79 ± 0.0434	486.4 ± 0.4
1	Y	N	7.59 ± 0.0459	467.7 ± 0.4
2	N	N	7.14 ± 0.0445	564.1 ± 0.4
2	Y	Y	5.78 ± 0.0401	577.3 ± 0.4
2	Y	N	7.25 ± 0.0449	562.8 ± 0.4
none	Y	Y	5.79 ± 0.0401	183.9 ± 0.3
none	Y	N	7.67 ± 0.0461	200.1 ± 0.2
Background			4.33 ± 0.0491	178.4 ± 0.3

Table 4.2: Neutron and gamma-ray rates measured by the planar detector for two containers, with ^{252}Cf-only and background measurements for comparison

Container	Poly?	Single Measurement	Combined Measurements	Agree?	Sigma
1	N	7.59 ± 0.0459	7.31 ± 0.0751	Y	3σ
1	Y	6.79 ± 0.0434	5.43 ± 0.0716	N	14σ
2	N	7.25 ± 0.0449	10.48 ± 0.0807	N	26σ
2	Y	5.78 ± 0.0401	8.60 ± 0.0775	N	25σ

Table 4.3: Comparison of neutrons rates measured with the planar liquid scintillator for container and source together ("Single Measurement" with rates measured for container and source separately ("Combined Measurements").

to the neutron background, the background measurements for the containers alone should be statistically consistent with the background. Third, the addition of the shielded ^{252}Cf source to Container 2 reduces the neutron rate to well below the rate measured for the container alone. The addition of a neutron source to the system should never result in a statistically significant reduction in counts.

The results of the consistency check are shown in Table 4.3. Only one set of measurements, for Container 1 with an unshielded source, produces results that are within 3 standard deviations of one another. The other three sets of measurements differ by between 14 and 26 standard deviations. These results, and the magnitude of the discrepancies, show that the planar detector, in combination with the pusle shape discrimination applied, was clearly behaving in an anomalous manner. Since the planar detector system fails basic performance criteria, it is not possible to produce a ROC curve for a scaled-up system.

5 Conclusions

Our conclusions following the measurement campaign remain essentially the same as our conclusions regarding liquid scintillators in the original report [1]. A standard portal monitor could hold 48 cylindrical liquid scintillator modules having dimensions of 3 inches in diameter and 3 inches high. It is left to the purchaser and supplier to assess the cost of this system. A comparison of the "innocent" alarm rate, defined as the probability of alarming on a container that does not contain a neutron source, is shown for the liquid-scintillator-based and SNAP-based systems in Figure 5.1. These are the innocent alarm rates for the particular cargo containers measured. Calculation of the overall innocent alarm rate due to gamma-ray misidentification using liquid scintillator based systems would require characterization of a representative set of containers, and weighting by their prevalance in commerce at a particular portal installation.

It has not been proven that a large-volume liquid scintillator can exhibit sufficiently uniform light output to perform in a portal monitor. This is not to say that it is impossible for a large-volume detector to do so, merely that the combination of the planar detector and software used in this measurement campaign were not able to behave in a consistent-enough manner to allow their performance to be assessed. Therefore, we must reiterate our original conclusion, that if there is a desire to develop liquid scintillators as an alternative to thermalizing detectors, then research into the design, construction, and characterization of large-volume liquid scintillators should be a priority.

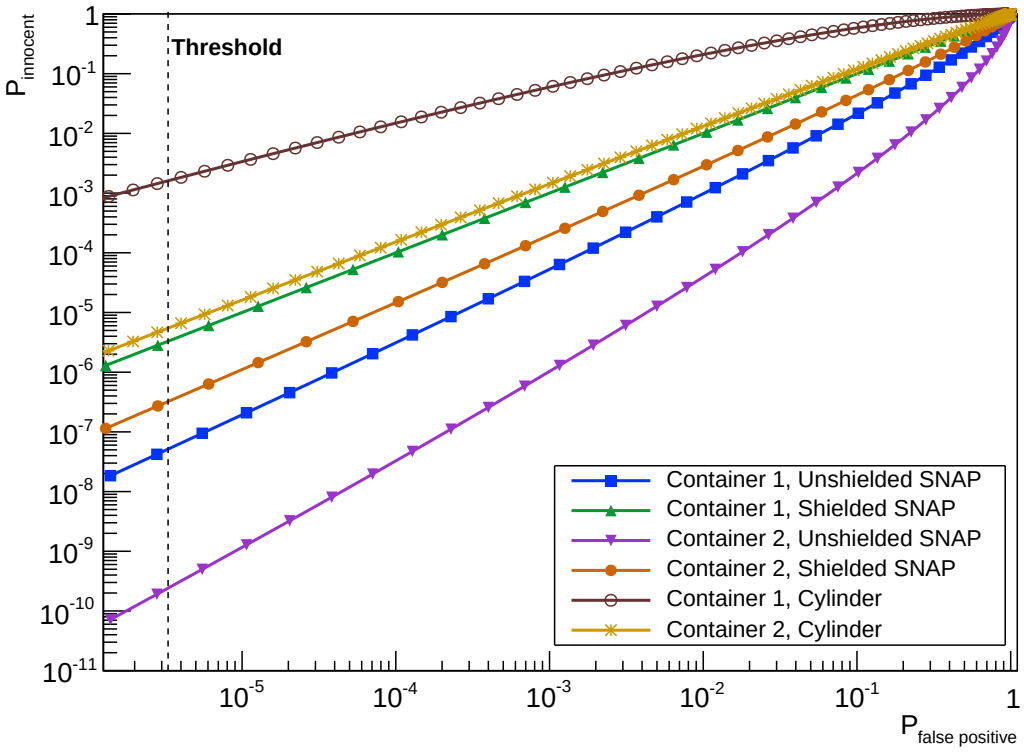

Figure 5.1: Probability of innocent alarm for different portal systems

Bibliography

[1] Edward A. McKigney and Sy Stange *Comparison of Fast Neutron Detector Technologies* Los Alamos National Laboratory, LA-UR-13-21178.

[2] National Committee on Radiation Instrumentation, N42 *American National Standard for Evaluation and Performance of Radiation Detection Portal Monitors for Use in Homeland Security* IEEE, New York, 2007 ANSI N42.35

[3] D. R. Mayo and R. B. Rothrock *Shielded Neutron Assay Probe (SNAP3)* Los Alamos National Laboratory, LA-UR-05-6818.